Decreased Interhemispheric Functional Connectivity in Autism

Jeffrey S. Anderson[1,2,3], T. Jason Druzgal[1], Alyson Froehlich[4], Molly B. DuBray[2,4], Nicholas Lange[5,6,7], Andrew L. Alexander[8,9], Tracy Abildskov[10,11], Jared A. Nielsen[2,4], Annahir N. Cariello[2,4], Jason R. Cooperrider[4], Erin D. Bigler[3,10,11] and Janet E. Lainhart[2,3,4]

[1]Department of Neuroradiology, [2]Program in Neuroscience, [3]The Brain Institute, [4]Department of Psychiatry, University of Utah, Salt Lake City, UT 84132, USA, [5]Department of Psychiatry, Harvard Medical School, 401 Park Drive, Boston, MA 02215, USA, [6]Department of Biostatistics, Harvard School of Public Health, 677 Huntington Avenue, Boston, MA 02115, USA, [7]Neurostatistics Laboratory, McLean Hospital, 115 Mill Street, Belmont, MA 02478, USA, [8]Department of Medical Physics, University of Wisonsin-Madison, 1111 Highland Ave, Madison, WI 53705, USA, [9]Department of Psychiatry, University of Wisconsin-Madison, 6001 Research Park Blvd, Madison, WI 53719, USA, [10]Neuroscience Center, Brigham Young University, 1055 SWKT, Provo, UT 84062, USA and [11]Department of Psychology, Brigham Young University, 1001 SWKT, Provo, UT 84062, USA

Address correspondence to Jeffrey S. Anderson, Department of Neuroradiology, University of Utah, 1A71 School of Medicine, Salt Lake City, UT 84132, USA. Email: andersonjeffs@gmail.com.

The cortical underconnectivity theory asserts that reduced long-range functional connectivity might contribute to a neural mechanism for autism. We examined resting-state blood oxygen level–dependent interhemispheric correlation in 53 males with high-functioning autism and 39 typically developing males from late childhood through early adulthood. By constructing spatial maps of correlation between homologous voxels in each hemisphere, we found significantly reduced interhemispheric correlation specific to regions with functional relevance to autism: sensorimotor cortex, anterior insula, fusiform gyrus, superior temporal gyrus, and superior parietal lobule. Observed interhemispheric connectivity differences were better explained by diagnosis of autism than by potentially confounding neuropsychological metrics of language, IQ, or handedness. Although both corpus callosal volume and gray matter interhemispheric connectivity were significantly reduced in autism, no direct relationship was observed between them, suggesting that structural and functional metrics measure different aspects of interhemispheric connectivity. In the control but not the autism sample, there was decreasing interhemispheric correlation with subject age. Greater differences in interhemispheric correlation were seen for more lateral regions in the brain. These findings suggest that long-range connectivity abnormalities in autism are spatially heterogeneous and that transcallosal connectivity is decreased most in regions with functions associated with behavioral abnormalities in autism. Autism subjects continue to show developmental differences in interhemispheric connectivity into early adulthood.

Keywords: autism spectrum disorders, brain development, fcMRI, fMRI, resting state fMRI

Introduction

Abnormalities in long-range, functional connectivity in autism have been demonstrated in multiple prior imaging studies (Castelli et al. 2002; Just et al. 2004, 2007; Koshino et al. 2005, 2008; Cherkassky et al. 2006; Kana et al. 2006; Kennedy et al. 2006; Kennedy and Courchesne 2008; Kleinhans et al. 2008). In paradigms involving working memory (Koshino et al. 2005, 2008; Mostofsky et al. 2009), executive function (Just et al. 2007), face processing (Kleinhans et al. 2008), motor function (Mostofsky et al. 2009), and language (Just et al. 2004; Kana et al. 2006), ASD individuals exhibited significantly decreased correlation between task-related regions of interest (ROIs).

Subsequently, resting state paradigms have shown atypical network properties of the default mode network (Kennedy et al. 2006; Kennedy and Courchesne 2008; Monk et al. 2009; Weng et al. 2009) and decreased functional connectivity of anterior/posterior projectional pathways (Cherkassky et al. 2006; Koshino et al. 2008). These observations and their relationship to observed differences in cytoarchitecture of the cortex are summarized in a theory of connectivity in autism characterized by local over connectivity but long-distance underconnectivity (Just et al. 2004; Courchesne and Pierce 2005; Geschwind and Levitt 2007; Casanova and Trippe 2009).

Structural imaging has also demonstrated abnormalities in long-range white matter pathways. Corpus callosal volume has been considered one index of interhemispheric connectivity (Manes et al. 1999; Hardan et al. 2000; Vidal et al. 2006; Keary et al. 2009). Decreased size of the corpus callosum is one of the most replicated structural findings in autism (Lainhart et al. 2005; Alexander et al. 2007; Stanfield et al. 2008; Keary et al. 2009). Diffusion tensor analysis of the corpus callosum demonstrated significant microstructural differences between autism and control groups in fractional anisotropy, mean diffusivity, and radial diffusivity (Alexander et al. 2007). Moreover, functional connectivity abnormalities have shown correlation with size of the genu, anterior portion, and total size of the corpus callosum in a theory of mind task (Mason et al. 2008) and with the genu in an executive function task in individuals with autism (Just et al. 2007).

Underconnectivity that is most specific to callosal (Alexander et al. 2007; Mason et al. 2008) projection pathways would be ideally measured by direct correlation between regions in the brain in corresponding positions in the opposite hemisphere, where transcallosal connectivity is greatest. Such a measurement might provide an excellent paradigm for evaluating long-range connectivity in the brain because interhemispheric connections have been shown to be among the strongest relationships observed with functional connectivity (Stark et al. 2008). Previous investigations of functional connectivity in autism have applied either ROI-based analyses (Just et al. 2004, 2007; Koshino et al. 2005, 2008; Kana et al. 2006; Kleinhans et al. 2008), task-based deactivation paradigms (Kennedy et al. 2006), or focused on a defined network, such as the default mode network (Di Martino et al. 2009; Monk et al. 2009; Weng et al. 2009).

To evaluate functional connectivity abnormalities in the corpus callosum, we examined high-functioning autism and typically developing control participants using resting-state *functional magnetic resonance imaging* (fMRI) (Biswal et al. 1995; Fox and Raichle 2007). We compared interhemispheric correlations between the autism and control samples to evaluate the spatial heterogeneity of interhemispheric connectivity abnormalities in autism. Based on structural, microstructural, and functional connectivity study findings to date, we hypothesized decreased interhemispheric correlations between homotopic cortical areas in the right and left hemispheres in autism.

Materials and Methods

Participant Selection

Fifty-three high-functioning adolescent and young adult males with autism spectrum disorders (all had autism except 1 Asperger syndrome and 3 PDD-NOS) were compared with 39 male typically developing control volunteers, group matched by age. Verbal IQ (vIQ), performance IQ (pIQ), handedness, autism diagnostic surveys, social responsiveness, and language function testing were obtained for most participants (Table 1). Two control subjects were ambidextrous, one control subject was left-handed, and 4 autism subjects were left-handed, and all of the remaining subjects were right-handed. Handedness did not differ significantly between the groups. The participants had no history of hearing problems; all had English as their first language.

As expected, language and motor function were impaired in the autism participants as a group. vIQ and pIQ scores showed small, but significant, decreases in the autism group. Language was significantly impaired in the autism group relative to the control group.

All experiments were undertaken with the understanding and written consent of each subject, with the approval of the University of Utah Institutional Review Board and in compliance with national legislation and the Code of Ethical Principles for Medical Research Involving Human Subjects of the World Medical Association.

Diagnosis and Exclusion Criteria

Diagnosis of autism was established in the majority of subjects by the Autism Diagnostic Interview-Revised (ADI-R) (Lord et al. 1994), Autism Diagnostic Observation Schedule-Generic (ADOS-G) (Lord et al. 2000), Diagnostic and Statistical Manual of Mental Disorders, Fourth Edition (DSM-IV) (American Psychiatric Association 1994), and International Statistical Classification of Diseases and Related Health Problems, 10th Revision (ICD-10) criteria. The diagnosis was established by an autism expert (J.E.L.) using the ADI-R and DSM-IV/ICD-10 criteria in 2 subjects and DSM-IV/ICD-10 criteria in 3 subjects. Individuals with medical causes of autism, identified by history, Fragile-X gene testing, karyotype, and examination, were excluded.

Control participants underwent tests of IQ, language, and neuropsychological function and were assessed with a standardized psychiatric interview (Leyfer et al. 2006). Most controls also were assessed with the ADOS-G (Lord et al. 2000) to confirm typical development. Controls with any history of developmental, learning, cognitive, neurological, or neuropsychiatric conditions were excluded.

Assessments

Handedness
The Edinburgh Handedness Inventory (Oldfield 1971), a standardized assessment of hand preference, was obtained for each subject. This inventory consists of a numerical score between −100 and 100, where −100 represents strong left-handedness and 100 represents strong right-handedness.

IQ
vIQ and pIQ were measured with the Wechsler Adult Intelligence Scale, WAIS III (Wechsler 1997) or Wechsler Abbreviated Scale of Intelligence, WASI (Wechsler 1999). The Differential Abilities Scale was used to test several children (Elliott 1990).

Language
Clinical Evaluation of Language Fundamentals—Third Edition (CELF-3) (Semel et al. 1995) was used to assess language skills. It is a comprehensive and nationally normalized clinical assessment tool that provides a quantitative measure of language level. The CELF-3 includes subtests that measure grammar, syntax, semantics, and working memory for language and provides an overall assessment of higher order receptive and expressive language and total language level.

Social Function
The Social Responsiveness Scale (SRS) is a normed, quantitative, 65-item rating scale that measures social impairments characteristic of autism spectrum disorders.

fMRI Acquisition
Images were acquired on Siemens 3 T Trio scanner. The scanning protocol consisted of initial 1-mm isotropic magnetization prepared rapid gradient echo (MP-RAGE) acquisition for an anatomic template. Blood oxygen level–dependent (BOLD) echoplanar images (time repetition = 2.0 s, time echo = 28 ms, Generalized Autocalibrating Partially Parallel Acquisition (GRAPPA) with acceleration factor = 2, 40 slices at 3-mm slice thickness, 64 × 64 matrix) were obtained during the resting state, where subjects were instructed to "Keep your eyes open and relax. Remain awake and try to let thoughts pass through your mind without focusing on any particular mental activity." Prospective motion correction was performed during BOLD imaging with PACE sequence (Siemens). An 8-min scan (240 volumes) was obtained for each subject.

Table 1

Characterization of control ($n = 39$) and autism ($n = 53$) populations

	Age	EHI	vIQ	pIQ	ADOS-S	ADOS-C	SRS	CELF-3
Autism subjects	53	53	53	53	48	48	47	51
Autism mean	22.4	65.1	101.3	101.3	8.9	4.7	89.4	88.0
Autism SD	7.2	46.9	21.1	16.5	2.5	1.4	32.7	22.2
Autism range	12–42	−93 to 100	55–139	67–134	1–14	1–7	6–147	50–121
Control subjects	39	35	34	34	29	29	31	32
Control mean	21.1	72.5	116.0	114.2	0.65	0.51	14.8	111.4
Control SD	6.5	33.8	14.8	13.9	0.89	0.68	11.5	11.42
Control range	8–34	−60 to 100	87–143	90–155	0–3	0–2	1–51	88–134
P value (2-tailed t-test)	0.36	0.42	**0.0006**	**0.0002**	**9.4×10^{-28}**	**2.3×10^{-23}**	**1.5×10^{-19}**	**4.3×10^{-7}**

Note: Summary statistics are provided for age, Edinburgh Handedness Inventory (EHI), vIQ (from either WASI or WAIS III), pIQ (from either WASI or WAIS III), Autism Diagnostic Observation Schedule-Social (ADOS-S) and Communication (ADOS-C) subtests, SRS, and CELF-3 (total score).

fMRI Postprocessing and Statistical Analysis

Offline postprocessing was performed in Matlab (Mathworks) using SPM8 (Wellcome Trust) software. Initial slice timing correction was performed to adjust for interleaved slice acquisition. Field map sequence was acquired for each subject for distortion correction, and all images were motion corrected using realign and unwarp procedure. BOLD images were coregistered to MP-RAGE anatomic image sequence for each subject. All images were normalized to Montreal Neurological Institute (MNI) template brain (T1.nii in SPM8).

Because BOLD images contain information not only from neural activity but also from physiological and artifactual sources such as respirations, heart rate, and scanner drift, more accurate connectivity measurements can be obtained by using a technique for removing global signal sources not associated with neural activity (Fox et al. 2009). Because physiological waveforms of heart rate and respiration were not available for all subjects during the scans, we used a regression algorithm using time series from voxels in the soft tissues, cerebrospinal fluid (CSF) and white matter to correct for artifactual correlations in the BOLD data (Fox et al. 2009). No global signal regression was performed to avoid introducing artifactual anticorrelations in the data (Murphy et al. 2009; Anderson, Druzgal, et al. 2010).

Scalp and facial soft tissues, CSF, and white matter regression were performed after automated gray matter, white matter, and CSF segmentation of each subject's MPRAGE image using SPM8. These segmented images were manually inspected to confirm appropriate identification of tissue components. The CSF time series for each subject was measured from the lateral ventricles. This was obtained from selecting voxels from the CSF segmented image for each subject within the bounding box defined by MNI coordinates: $-35 < x < 35$, $-60 < y < 30$, $0 < z < 30$. White matter time series for each subject were obtained from the mean time series of voxels within 2 ROIs in the bilateral centrum semiovale (MNI coordinates: left: $x = -27$, $y = -7$, $z = 30$; right: $x = 27$, $y = -7$, $z = 30$, each ROI had 10-mm radius). Before extracting the white matter time series, an exclusive mask was performed with the gray matter segmented image from each subject to eliminate voxels containing gray matter. A soft tissue mask of the facial and scalp soft tissues was used as previously described (Anderson, Druzgal, et al. 2010). The mean soft tissue, CSF, and white matter time series were then used as regressors in a general linear model (glmfit.m in Matlab Statistics Toolbox) for the BOLD time series at each voxel in the brain, and the best fit was subtracted from the voxel's time series data, producing the signal-corrected time series images. Each voxel's time series was band-pass filtered with a frequency window of 0.001–0.1 Hz (Cordes et al. 2001) and linearly detrended to correct for scanner drift. These images were used for subsequent analysis.

Interhemispheric Correlation

For each subject, the time series at each voxel in the image was computed and a corresponding voxel in the opposite hemisphere was obtained by inverting the MNI space x coordinate. A cross-correlation curve was computed between each pair of time series, and the zero lag correlation (equivalent to Pearson correlation coefficient) was used to construct an image of interhemispheric correlation (Fig. 1). This image was converted using Fisher Z-transformation by computing the hyperbolic arctangent of the value of each voxel to obtain an image of Z-scores for correlation (Kennedy and Courchesne 2008; Fox et al. 2009; Murphy et al. 2009). Because there are small variations in gray matter anatomy between the left and right hemispheres, these interhemispheric Z-score images were spatially smoothed to mitigate noise in the images using SPM8 (full-width at half-maximum of $8 \times 8 \times 8$ mm).

Histograms of interhemispheric correlation distribution were computed for gray matter voxels by using a binary mask obtained from SPM8 gray.nii image. The same gray matter mask was used for all subjects in this step so the same number of voxels was used for each subject's normalized data. Histograms and 95% confidence intervals were computed on z-transformed values.

Interhemispheric correlation images after Fisher's z-transform (Lowe et al. 1998) were used for a second-level analysis comparing autism and control groups using SPM8, in which a 2-tailed t-test design was used to calculate significance of the interhemispheric correlation differences
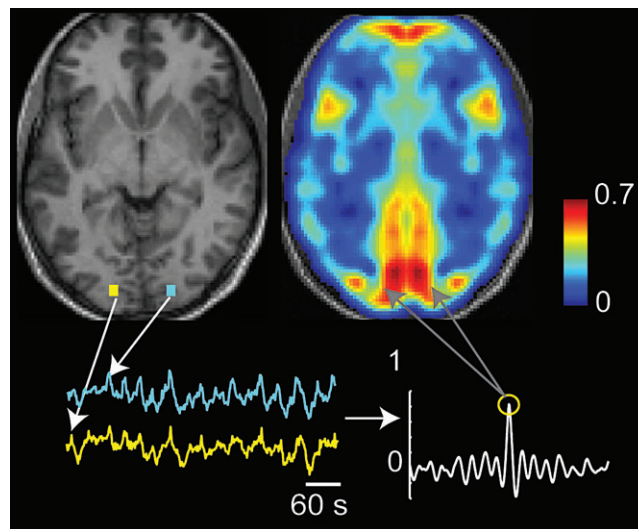
Figure 1. Calculating interhemispheric correlation. For each voxel in the image, a corresponding voxel in the opposite hemisphere was obtained by inverting the MNI x coordinate. Time series for each pair of voxels was obtained, and the value of the cross-correlogram at zero lag (Pearson correlation coefficient) was used to construct an image of interhemispheric correlation. This image was Fisher transformed by evaluating hyperbolic arctangent and then spatially smoothed.

between autism and control samples. The second-level analysis was repeated using neuropsychiatric and demographic covariates of age, vIQ, pIQ, language (CELF-3 total score), SRS, ADOS-G algorithm score (sum of social and communication scores), and handedness as covariates. Analysis was performed with each metric individually in the general linear model, as well as with all metrics combined into a single general linear model.

Calculation of Corpus Callosal Volume

Cortical reconstruction and volumetric segmentation were performed with the FreeSurfer image analysis version 4.0.4 (Athinoula A. Martinos Center for Biomedical Imaging, 2005). Details of the procedures are described in prior publications (Dale and Sereno 1993; Dale et al. 1999; Fischl, Sereno, and Dale 1999; Fischl and Dale 2000; Fischl et al. 2001, 2002; Han et al. 2006; Jovicich et al. 2006). Briefly, nonbrain tissue was removed using a hybrid watershed/surface deformation procedure (Segonne et al. 2004), automated Talairach transformation, segmentation of the subcortical white matter (WM) and deep gray matter (GM) volumetric structures (Fischl et al. 2002, 2004), intensity normalization (Sled et al. 1998) tessellation of the GM-WM boundary, automated topology correction (Fischl et al. 2001; Segonne et al. 2007), and surface deformation following intensity gradients to optimally place the GM/WM and GM/CSF borders at the location where the greatest shift in intensity defines the transition to the other tissue class (Dale and Sereno 1993; Dale et al. 1999; Fischl and Dale 2000). The resulting cortical models were registered to a spherical atlas, utilizing individual cortical folding patterns to match cortical geometry across subjects (Fischl, Sereno, Tootell, et al. 1999). The cerebral cortex was parcellated into regions based on gyral and sulcal structure (Desikan et al. 2006). Results for each subject were visually inspected to ensure accuracy of registration, skull stripping, segmentation, and cortical surface reconstruction. Corpus callosal volumes of posterior, mid posterior, mid, mid anterior, and anterior corpus callosum were added to produce a total corpus callosal volume for each subject used in subsequent analyses.

Results

The procedure used in constructing maps of interhemispheric correlation is illustrated in Figure 1, where the value at each
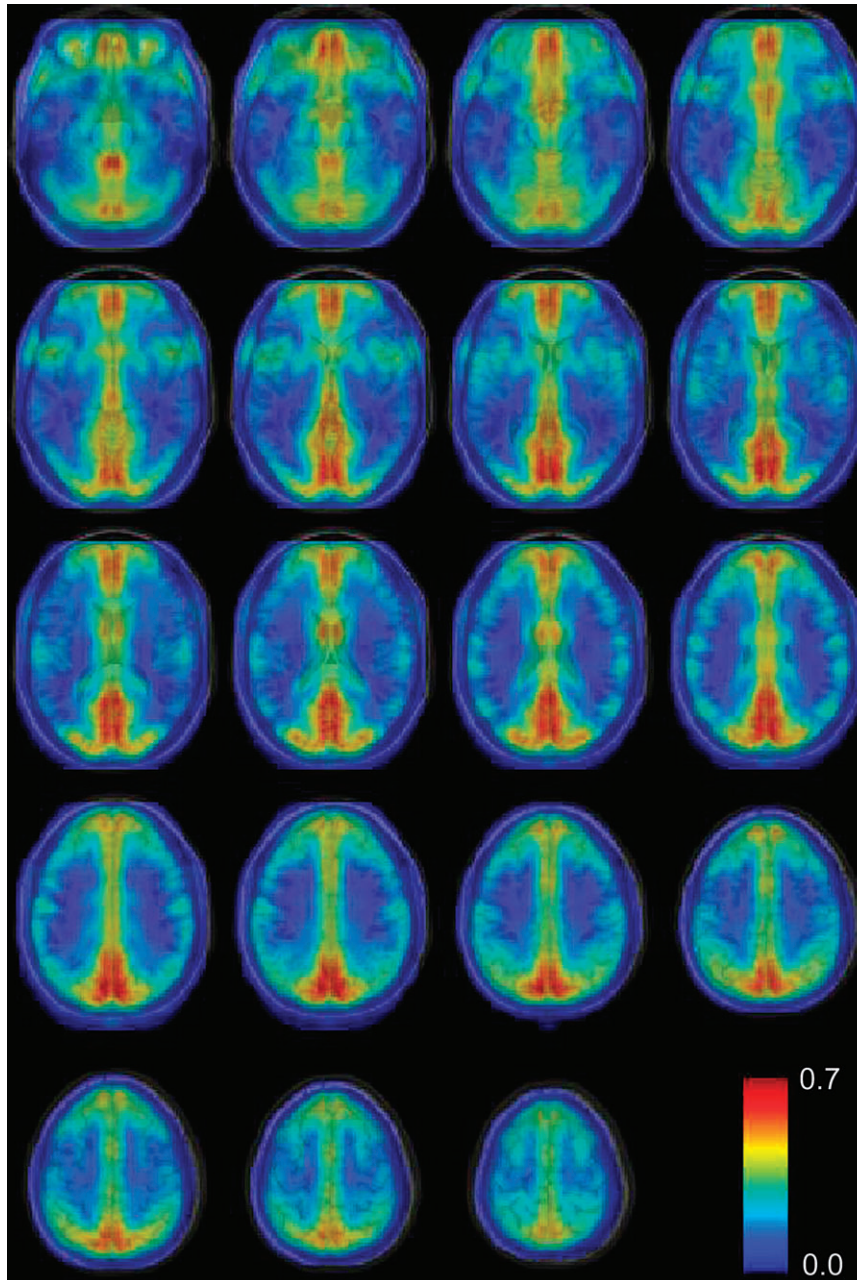
Figure 2. Interhemispheric correlation averaged over 39 control subjects. Scale bar shows Fisher-transformed correlation (*Z*-score).

voxel represents the correlation coefficient between the time series at that voxel and the corresponding voxel in the opposite hemisphere. Such interhemispheric correlation maps showed reproducible patterns of interhemispheric correlation at the single subject level. These patterns are shown in Figure 2, in which *Z*-transformed maps of interhemispheric correlation were averaged from 39 control subjects, overlaid on a canonical MNI-normalized MP-RAGE image.

Interhemispheric Correlation in Typical Development

We first characterized the spatial distribution of voxelwise interhemispheric correlation in the control population. The group map of interhemispheric correlation in control subjects shows spatial heterogeneity, consistent with the ROI technique

for interhemispheric correlation observed in a prior study (Stark et al. 2008) and similar to results obtained using a related voxelwise technique to study age-related changes in interhemispheric correlation (Zuo et al. 2010). First, interhemispheric correlations appear higher among gray matter voxels than white matter voxels, as would be expected if interhemispheric correlation is a measure of synchronized underlying neural activity in areas of relatively higher anatomic connectivity. It is also possible that this reflects our postprocessing strategy of CSF and white matter regression because mean brain signal or gray matter signal was not regressed, but this is considered unlikely because a similar pattern was seen in interhemispheric correlation results from data before they were subjected to the regression postprocessing technique.

Interhemispheric correlation appears higher for voxels closer to the midline. Relatively higher values of correlation are seen in the frontal pole, occipital cortex and medial parietal lobe, deep gray nuclei, and cerebellum, all of which are relatively close to the midline. The trend toward higher connectivity near the midline does not apply uniformly, however. Areas of lateral sensorimotor cortex, visual cortex, primary auditory cortex, and the anterior insula show, for example, greater correlation than surrounding brain structures of similar distance to the midline. Higher connectivity in sensorimotor areas might be expected given known strong thalamocortical contributions in these areas, with shared inputs from sensory and motor signals that exhibit left/right symmetry. Common inputs from the thalamus might be expected to produce greater synchronization in activity. Given these patterns, interhemispheric correlation appears consistent with known underlying anatomical connectivity. Similar spatial heterogeneity was observed in the group map of interhemispheric correlations in the autism group.
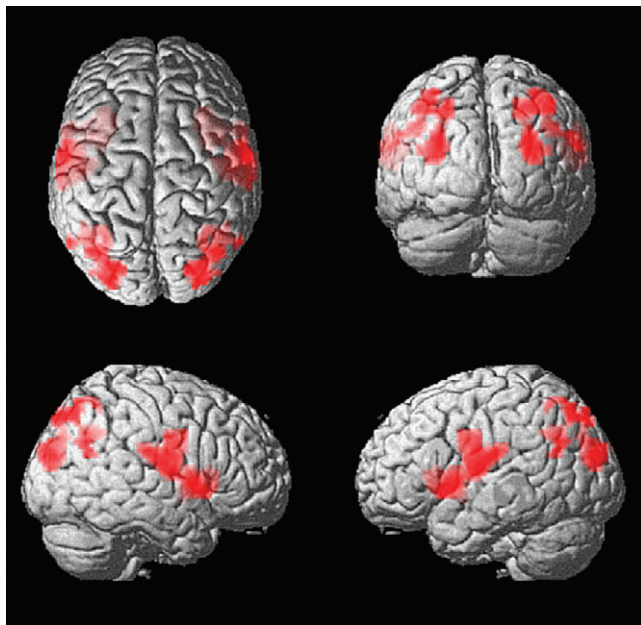
Figure 3. Control > autism interhemispheric correlation. Regions of greater interhemispheric correlation for 39 controls than in 53 autism subjects. All clusters were significant at $q < 0.001$, false discovery rate. No voxels showed significantly greater interhemispheric correlation for autism than control subjects.

Table 2
Peak MNI coordinates of control > autism interhemispheric correlation

Region	x	y	z	T score	Number of voxels	Cluster-level q score (FDR)
Anterior insula	33	14	1	5.1	574	0.00001
Lateral sensorimotor cortex	51	−13	19	4.2		
Lateral sensorimotor cortex	60	−10	13	4.1		
Lateral parietooccipital junction	30	−88	19	4.6	305	0.0008
Posterior superior parietal	30	−82	49	4.4		
Intraparietal sulcus	39	−76	49	4.4		

Note: Significant results fell in an anterior (insula, lateral sensorimotor) and a posterior (superior parietal lobule) cluster.
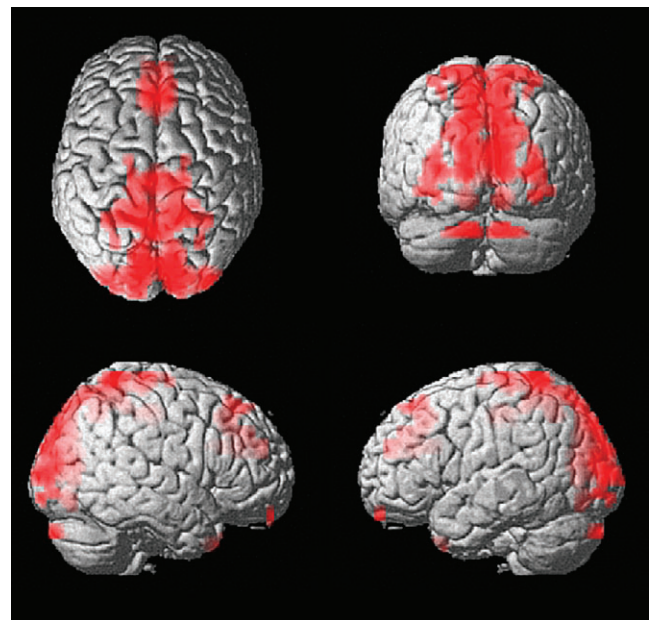
Differences in Interhemispheric Correlation in Autism

Interhemispheric correlation shows a trend toward lower values in autism throughout the brain, but some areas are affected more than others. Figure 3 shows regions where control subjects showed significantly higher interhemispheric correlation than autistic subjects, with all clusters significant at an acceptable false discovery rate $q < 0.001$. Peak coordinates for significant clusters are listed in Table 2. No voxels showed significantly higher correlation for autistic subjects than control subjects. Regions showing higher interhemispheric correlation for control subjects include sensorimotor cortex, frontal insula, and superior parietal lobule extending from the parietooccipital junction to the intraparietal sulcus.

Differences in interhemispheric correlation in autism do not merely occur in areas of highest interhemispheric correlation in the control population. Rather, many areas with high correlation, such as visual cortex, medial frontal lobes, and striatum, do not show significant differences between autism and control samples. Moreover, the effect is also not well described by changes only to voxels of intermediate connectivity, as might be seen if the effect were due to a greater dynamic range among subjects in voxels with intermediate correlation. Many areas in this range do not show group differences, such as dorsolateral prefrontal cortex and caudate nuclei, among others. Differences in interhemispheric connectivity also show poor match to spatial distribution of physiological confounds, such as cerebral blood volume and respiratory variation (Birn et al. 2006, 2008).

Covariates and Interhemispheric Correlation

To account for factors other than diagnosis that might underlie these regional differences in interhemispheric correlation, we included in a general linear model covariates of age, vIQ, pIQ, language total score (CELF-3), SRS, ADOS-G algorithm score, and handedness. Regions showing control greater than autism

Figure 4. Increased interhemispheric correlation associated with younger age. All clusters were significant at $q < 0.001$, false discovery rate. No voxels showed significantly higher interhemispheric correlation with older age or higher or lower vIQ, pIQ, Edinburgh Handedness Inventory, ADOS, SRS, or CELF-3 scores.

interhemispheric correlation remained significant when these factors were included as regressors in the model. Each covariate was analyzed separately with diagnosis as well as in a combined general linear model with all of the covariates. In each case, the only covariate that showed significant associations with interhemispheric correlation was age, shown in Figure 4. Younger subjects showed higher interhemispheric correlation near the midline, particularly in the supplementary motor area, precuneus, and occipital lobe.
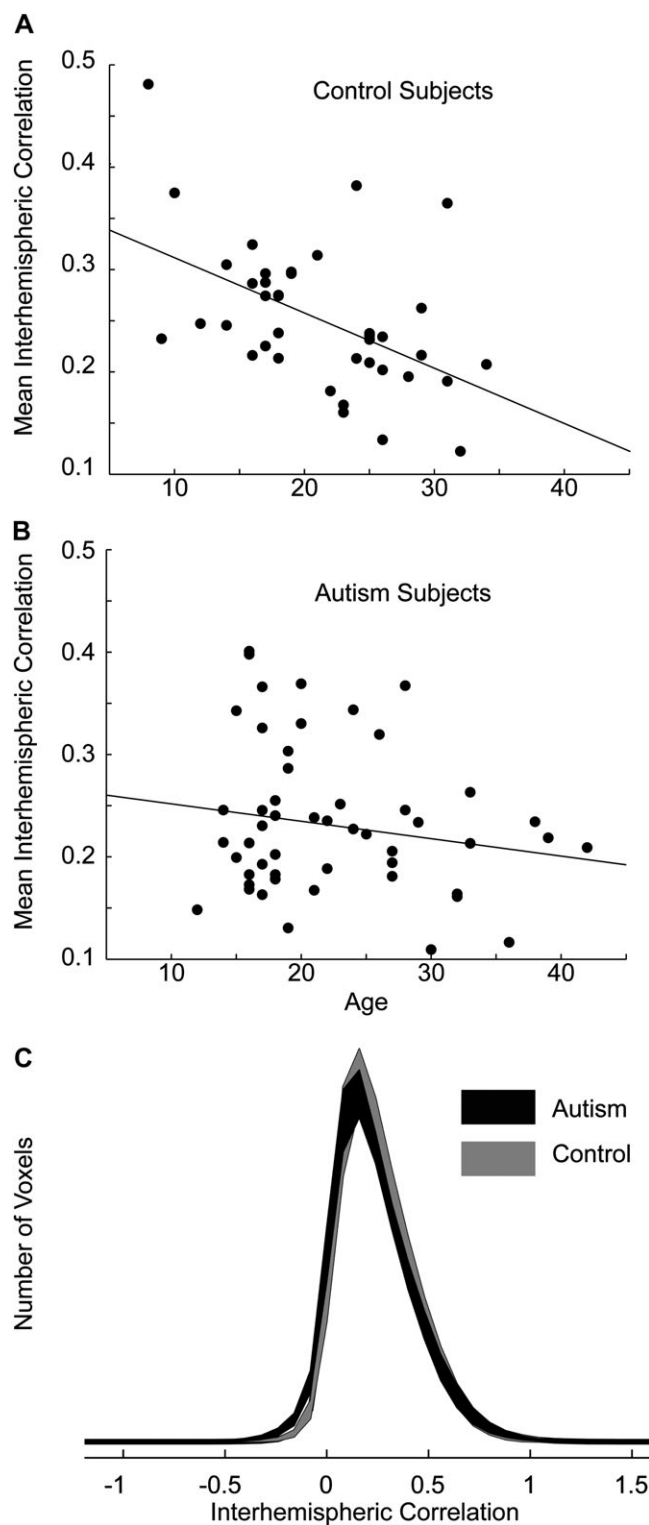
Mean Interhemispheric Correlation and Age

We obtained an estimate of mean interhemispheric correlation by averaging overall gray matter voxels within the interhemispheric correlation images for each subject. Mean gray matter interhemispheric correlation was reduced in the autism sample relative to the control sample (control 0.253 ± 0.071 standard deviation [SD], autism 0.232 ± 0.071 SD) To evaluate the significance of this difference, we included age as a covariate because a significant relationship was seen in the voxelwise analysis of Figure 4. Using a general linear model with diagnosis and age as regressors and including an interaction term, we confirmed the hypothesis that control subjects showed significantly higher interhemispheric correlation than autism subjects ($P = 0.023$, one-tailed t-statistics), with a significant interaction between age and diagnosis ($P = 0.043$). This is illustrated in Figure 5, showing greater decreases in mean interhemispheric correlation with age among control subjects than among autism subjects.

The changes seen in interhemispheric correlation appear most significant among the younger subjects. We divided our autism and control samples into subjects younger than or equal to age 20 and subjects older than 20. In the younger control group, the correlation with age was significant ($r = -0.48$, $P = 0.019$, one-tailed t-test). In the older group, the correlation was not significant ($r = -0.09$, $P = 0.36$). In the autism sample, neither the younger group ($r = 0.03$, $P = 0.43$) nor the older group ($r = -0.22$, $P = 0.15$) showed a significant correlation between mean interhemispheric correlation and age. In the combined autism and control sample, no voxels showed a significant relationship with one-tailed t-tests between mean interhemispheric correlation and neuropsychological metrics of vIQ ($r = -0.09$, $P = 0.19$), pIQ ($r = 0.05$, $P = 0.31$), handedness ($r = -0.11$, $P = 0.16$), Autism Diagnostic Observation Schedule-Social ($r = -0.03$, $P = 0.40$), Autism Diagnostic Observation Schedule-Communication ($r = -0.09$, $P = 0.23$), or language function testing ($r = -0.01$, $P = 0.45$) in our data. SRS scores showed a strong trend toward decreased social impairment with higher mean interhemispheric correlation ($r = -0.18$, $P = 0.058$).

Corpus Callosum Volume and Interhemispheric Correlation

Corpus callosum mean volume was significantly reduced in the autism sample relative to the control sample (control 3523 ± 450 SD, autism 3271 ± 600, one-tailed t-test, $P = 0.015$). In order to evaluate the relationship of functional interhemispheric correlation with callosal volume, we compared the mean gray matter interhemispheric correlation values for each subject with total corpus callosal volume and found no significant correlation ($r = -0.009$, $P = 0.93$). No significant correlation was seen in either the autism or control sample between gray
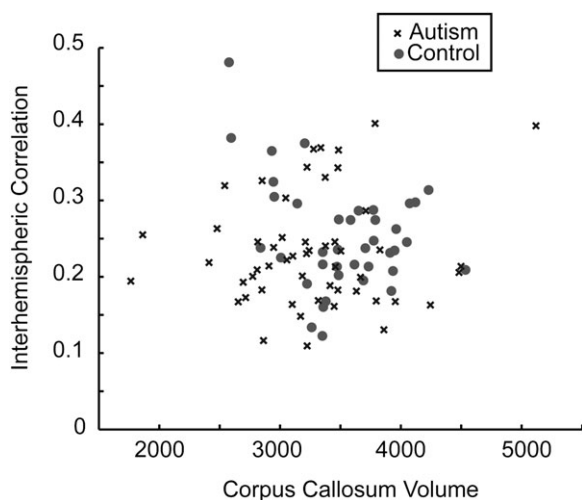

Figure 5. Relationship of mean gray matter interhemispheric correlation with subject age. (A) Each point represents mean gray matter interhemispheric correlation for 1 of 39 control subjects (above), with best straight line fit through the data. (B) The same is shown below for 53 autism subjects. (C) Distributions of interhemispheric correlation across gray matter voxels. Distributions were computed for each subject and shaded averages above show pointwise 95% confidence intervals for distributions from autism and control populations, computed on Fisher-transformed correlation.
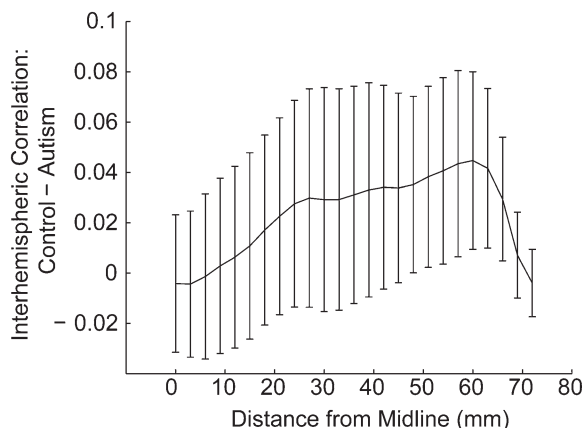
matter functional interhemispheric correlation and corpus callosal volume when samples were analyzed separately. These data are shown in Figure 6.

Interhemispheric Correlation and Distance from Midline

Voxelwise data showed significant differences in interhemispheric correlation in autism were lateral to the midline. To evaluate whether interhemispheric correlation in autism is related to a voxel's position on the medial–lateral axis, we computed the difference in mean interhemispheric correlation for each voxel between the control and autism samples and averaged this value for all gray matter voxels in each sagittal slice, shown in Figure 7. There is increasing interhemispheric correlation for control subjects relative to autism subjects with distance from the midline with a peak at 60 mm. Greater than one SD of gray matter voxels at this distance show greater interhemispheric correlation for control subjects, while essentially no difference in interhemispheric correlation is seen at the midline.

Alternate Method: Regional Parcellation

Another method for calculating interhemispheric correlation was used in addition to the voxelwise technique described above. The supratentorial brain was parcellated into 90 regions using the AAL brain atlas (Tzourio-Mazoyer et al. 2002; Maldjian et al. 2003). These consist of 45 left/right homologous regions. For each region, the mean BOLD time course was extracted for each subject, and correlation was compared with the homologous region in the opposite hemisphere, similar to a method previously used to measure interhemispheric correlation (Stark et al. 2008). While this method has lower spatial resolution, it might also be less sensitive to noise present in the voxelwise method.
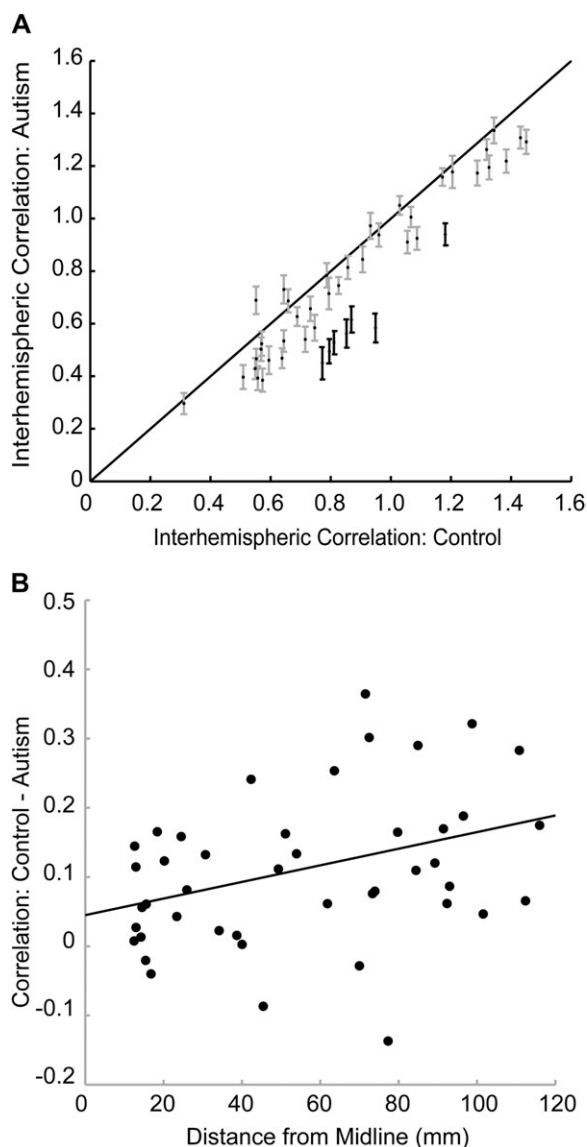
Figure 6. Interhemispheric correlation does not vary with corpus callosal volume. Mean interhemispheric correlation of gray matter voxels is compared with corpus callosal volume from the MP-RAGE scan for each subject.

Figure 7. Differences in interhemispheric correlation increase with distance from the midline. The difference of mean interhemispheric correlation from gray matter voxels between control and autism subjects is shown for each sagittal slice. Error bars represent SD across voxels in the slice for difference in mean correlation between control and autism samples.

Figure 8. Effect of distance between regions on interhemispheric correlation. (*A*) The supratentorial brain was parcellated into 45 pairs of left/right homologous regions. Each point shows the mean interhemispheric correlation between left and right homologues for one region. Error bars show standard error of the mean across autism subjects. Dark bars were statistically significant after Bonferroni correction. (*B*) The same regions as above were used to plot the difference between control and autism mean interhemispheric correlation for each region against the Euclidean distance between the centroids of the left and right homologues for the region.

Mean control and autism population values for each region are shown in Figure 8. Forty of the 45 regions showed greater interhemispheric correlation for controls. This was statistically significant across subjects after multiple comparison correction in 7 regions: rolandic operculum, insula, superior and mid occipital, fusiform, postcentral, and superior temporal. These are largely the same regions seen in the voxelwise analysis of Figure 3. Strong trends in the fusiform gyrus and superior temporal gyrus were also seen in the voxelwise data. When the distance from midline was measured from the centroid of each region, there was again a significant trend toward greater interhemispheric correlation in controls with distance from the midline ($r = 0.35$, $P = 0.009$).

Discussion

We report regionally specific decreases in interhemispheric correlation in autism subjects compared with typically developing controls. The resting-state fMRI interhemispheric correlational differences in autism were localized to sensorimotor cortex, superior parietal lobule, frontal insula, superior temporal gyrus, fusiform gyrus, and perisylvian posterior inferolateral premotor cortex. Interhemispheric correlation differences were more associated with the diagnosis of autism than with quantitative measures of IQ, language function, and handedness. Significant age-related decrease in mean interhemispheric correlation observed in controls was absent in the group with autism.

Resting-State fMRI Interhemispheric Correlations

Correlation of the fMRI BOLD time series of gray matter is believed to be an indirect index of synchrony in spontaneous neural activity and likely related to the intrinsic functional architecture of the brain (Biswal et al. 1995, 2010; Fox and Raichle 2007; Buckner et al. 2009). In response to stimuli, animals have coherent fluctuations in electrical activity in cortical neurons that are connected interhemispherically, and fluctuations in electrical activity and BOLD hemodynamic responses are statistically associated (Innocenti 2009). Similar to interhemispheric electroencephalography coherence, the degree of correlation in the BOLD time series between 2 regions at rest is used as an estimate of the strength of their baseline, nontask–related functional connectivity. It is important to note, however, that a variety of factors other than spontaneous neural activity can affect the observed correlations (Jones et al. 2010). The importance of understanding interregional correlations in spontaneous neural activity has been recently emphasized. Observed correlations in fMRI time series between brain regions during performance of a task and autism-control differences in the correlations are likely driven by fluctuations in neuronal activity that are unrelated to the task (Jones et al. 2010).

Regionally Specific Decreased Interhemispheric Correlations in Autism

We found an overall decrease in the correlation of the time series in homologous voxels in the 2 hemispheres in the autism sample, with greatest effect seen in areas of the brain relevant to clinical abnormalities observed in autism. The largest difference in correlation observed was in the anterior (frontal) insula. The frontal insulae are core components of social processing networks and constitute a hub mediating integra-

tion of external and internal stimuli with consistent hypoactivity in autism studies (Uddin and Menon 2009). Frontoinsula is also a core region of the recently described salience network involved in identification of novel or relevant stimuli across sensory modalities (Seeley et al. 2007). The left frontoinsular region was specifically hypoactive in autism subjects in a study of novelty detection using an auditory oddball paradigm (Gomot et al. 2006).

Superior temporal gyrus has been implicated as a site of abnormal auditory processing in autism, as well as a locus associated with social intelligence. An fMRI study of social intelligence reported activation of superior temporal gyrus during processing of social judgments (Baron-Cohen et al. 1999). Volumetric studies have shown atypical structure–function relationships suggesting abnormal lateralization of superior temporal gyrus in autism (Bigler et al. 2007). Abnormalities of white matter microstructure in the superior temporal gyrus, detected by diffusion tensor imaging of autism, include significantly decreased fractional anisotropy and increased mean and radial diffusivity (Lee et al. 2007). Auditory processing of rapid (Oram Cardy et al. 2005) and steady-state (Wilson et al. 2007) stimuli, known to involve the superior temporal gyrus, was found to be abnormal in autism subjects using magnetoencephalography analysis. A recent fMRI study of language processing showed hypoactivity in autism at the junction of the superior temporal gyrus and left posterior insula (Anderson, Lange, et al. 2010), a locus included in the abnormal superior temporal gyrus interhemispheric correlation cluster.

Other areas of reduced interhemispheric connectivity in autism included primary sensorimotor and lateral inferior premotor cortex. This finding might be related to well-known gross and fine motor skill impairments associated with autism (Vilensky et al. 1981; Frith 1991; Jansiewicz et al. 2006; Mostofsky et al. 2009). Alteration in the volume of white matter deep to primary motor cortex correlates with greater impairment in basic motor skills in children with autism (Mostofsky et al. 2007). Impairments in basic motor control are among the earliest deficits observed in some infants who develop autism (Brian et al. 2008; Zwaigenbaum et al. 2009). Lower correlations involving the superior parietal lobule in autism were observed in a study of the functional connectivity of residuals after the effects of task response were removed (Jones et al. 2010).

Abnormalities in function in the fusiform gyrus are also reported in the literature in the context of social function and face processing in autism (Pierce and Redcay 2008; Corbett et al. 2009). Functional connectivity of the fusiform gyrus to frontal regions has been reported to be lower in autism during facial processing tasks (Kleinhans et al. 2008; Koshino et al. 2008). A postmortem study in 7 autism patients and 10 controls showed decreased numbers of neurons specifically in the fusiform gyrus in autism (van Kooten et al. 2008).

If autism is manifest by an overabundance of short-range connections and impaired long-range connections (Casanova and Trippe 2009), this can also be seen as a failure of the segregation and integration process. Segregation is thought to involve pruning of local connections, whereas integration involves strengthening of long-range connections within distributed functional networks (Fair et al. 2007, 2009). The regions where our data show greater interhemispheric

connectivity are precisely those that are longer-range, more lateral (lateral sensorimotor and premotor but not medial), and in areas of association cortex, such as superior parietal lobule, frontal insula, and posterior lateral frontal lobe, which are more likely to be strengthened during integration. This hypothesis would also explain functional connectivity results obtained during a Go/No Go task where connectivity from inferior frontal gyrus to supplementary motor area showed greater differences with age between autism and control samples, as would be expected from delayed or impaired integration (Lee et al. 2009).

Age-Related Changes in Interhemispheric Correlations

We report atypical age-related changes in interhemispheric correlations in autism. Across the age range we studied, 8–42 years, control subjects showed decreasing interhemispheric correlations, particularly in medial cortical regions. The autism subjects showed much less change with age, and the relationship was not statistically significant either in the younger (less than 20 years) or older subgroups. The relative lack of age-related changes in the autism group appeared to be driven by abnormally decreased interhemispheric correlations in a substantial subgroup of younger individuals and to a lesser extent somewhat increased interhemispheric correlations relative to controls in a small subgroup of older individuals. A diffusion tensor study of the corpus callosum, the main interhemispheric tract, found a similar pattern between 7 and 33 years of age: significant age-related changes in total corpus callosum volume, fractional anisotropy, and radial diffusivity present in typically developing controls were absent in the autism group (Alexander et al. 2007). Although caution is required when making inferences about developmental processes from cross-sectional data (Kraemer et al. 2000), the combined findings suggest a hypothesis that needs to be tested with longitudinal data: that the developmental trajectory of interhemispheric connectivity deviates from typical development in a nonlinear manner from childhood into adulthood in autism and is related to aberrant tensor scalar measures of corpus callosum microstructure. Abnormalities of interhemispheric connectivity in childhood and different abnormalities in adulthood provide additional support to a growing body of literature that suggests brain development during late as well as early childhood and brain maturation during young adulthood are abnormal in autism.

Our finding is particularly important in the developmental context of maturing connectivity during late adolescence and early adulthood. The brain has been shown to undergo segregation and integration across development (Varela et al. 2001; Fair et al. 2007; Supekar et al. 2009), where segregation corresponds to specificity of neural function in local spatial regions and integration represents development of relationships between spatially disparate regions in the brain with related function. For example, default mode regions are only sparsely connected in childhood and strengthen with age (Fair et al. 2008). In other networks, a similar pattern is seen where correlated ensembles develop locally first, with distributed networks occurring in adolescence or early adulthood (Fair et al. 2009). Using independent component analysis to define networks, it has also been shown that distributed networks show increasing efficiency and less mutual interdependence with age (Stevens et al. 2009). These data suggest

a neurodevelopmental mechanism of overconnectivity followed by pruning or weakening of short-range functional connections. Our data in typically developing controls are consistent with these results in that connections near the midline showed decreased interhemispheric correlation with age.

A prior study evaluating corpus callosal microstructure found increased fractional anisotropy with age in controls but not in autism subjects. This is curious in that in the present study mean gray matter interhemispheric correlation decreases with age. To reconcile these findings, we note that the decrease in correlation was driven by more medial voxels such as the ones showing greatest association with age in Figure 4. It is possible that in these voxels decreasing correlation might represent the effects of integration, where midline structures are increasingly connected to other distant brain regions with age (such as default mode and attention control networks) and that these strengthened connections represent a greater proportion of the variance of the BOLD signal, lowering the interhemispheric synchrony for midline regions. Also possible is that interhemispheric correlation measures features of connectivity not directly related to colossal projections (particularly given the absence of direct correlation between corpus callosal volume and interhemispheric correlation that we found), such as shared input from the thalamus or subcortical structures.

Corpus Callosum Volume and Interhemispheric Correlations

Compared with typically developing controls, our autism sample had decreased mean total corpus callosum volume and a decrease in the overall mean correlation of time series in homologous interhemispheric gray matter voxels. These findings are consistent with replicated findings of decreased callosal size (Manes et al. 1999; Chung et al. 2004; Waiter et al. 2005; Vidal et al. 2006; Freitag et al. 2009; Keary et al. 2009) and fractional anisotropy of white matter (Alexander et al. 2007; Keller et al. 2007; Brito et al. 2009) in the corpus callosum. Size decreases in the corpus callosum have been shown to be correlated with neuropsychological abnormalities in a motor task in autism (Keary et al. 2009), frontoparietal functional underconnectivity (Just et al. 2007), and reduced gyral window, consistent with minicolumnar findings in the cortex in autism and a bias toward local relative to long-range connectivity (Casanova et al. 2009).

Corpus callosum volume and interhemispheric resting-state time series correlation of homologous voxels were not related within individuals in our sample. The tendency toward smaller corpus callosum volume and decreased interhemispheric correlation might be biologically independent phenomena, at least at the level of the total corpus callosum and overall mean connectivity. This finding is in contrast to studies of functional connectivity between intrahemispheric and interhemispheric cortical areas during the performance of neuropsychological tasks. These studies have found significant positive correlations between size of the total corpus callosum or its subregions and functional connectivity in autism samples but usually not in controls. Based on the findings, it has been proposed that corpus callosum volume or mid-sagittal area constrains task-related functional connectivity.

Our findings suggest that corpus callosum volume, although decreased in autism, is associated but not correlated with decreased interhemispheric functional connectivity between homologous gray matter voxels in the resting state. The functional information we describe might characterize different aspects of connectivity not present in volumetric data alone. Volumetric and diffusion tensor measurements of white matter only relay information on white matter axonal architecture in the corpus callosum and not differences related to synaptic efficiency or number that can affect functional correlation. In addition, the interhemispheric correlations we observed might not reflect transcallosal connectivity but rather shared inputs from other sources. The mechanism for correlation might be more complicated, possibly involving corticostriatal, corticothalamic, or corticocerebellar pathways. It is also possible that other commissural fibers such as the fornix or anterior commissure contribute to interhemispheric correlation. Correlation with diffusion imaging and other metrics of white matter microstructure might help determine the extent to which transcallosal connections drive the high functional connectivity we observed in controls and the differences we found in autism.

Alternative Explanations for Observed Decreased in Interhemispheric Correlation in Autism

It is possible that the abnormalities we observed in interhemispheric connectivity in autism arose from case-control differences other than a primary deficit in correlated spontaneous neural activity in homologous gray matter voxels. The decreased correlations could be the secondary result of atypical experience rather than a primary component of the neural mechanism of autism. Case-control differences in cognitive and behavioral characteristics might have confounded the results. Yet, across multiple neuropsychological indices, correlation abnormalities were more associated with diagnosis of autism than other metrics. It is not yet known if the increased rates of macrocephaly and megalencephaly in autism affect structural and functional connectivity. In evolution, larger brains are associated with increased cortical volume and folding, decreased corpus callosum size relative to total brain volume, decreased interhemispheric connectivity, and increased intrahemispheric functional specialization (Casanova et al. 2009). But enlarged brain volume appears to be mainly a phenomenon of early childhood in autism, with mean brain volume not differing significantly from typical in older individuals with the disorder (Lainhart et al. 2005). The differences in interhemispheric correlation of homologous voxels could result from functionally different neurons in homologous voxels in cases and controls. Intersubject and interhemispheric variability exist in how cytoarchitectonic functional areas map onto MRI-defined voxels (Scheperjans et al. 2008). If variability is systematically increased in autism (Muller et al. 2003; Bailey et al. 2005), and resting-state interhemispheric connectivity is stronger between functionally related areas than between structurally homologous areas, decreased correlation between fMRI time series in homologous voxels could result from differences in variability of structure–function maps between groups. Even if this is the case in our samples, the findings would still suggest that increased interhemispheric structure–function variability is not uniform in autism but occurs in specific areas relevant to core and associated features of the disorder.

Finally, resting-state examinations are difficult to control, given the relatively unconstrained mental activity that occurs. Interindividual variations in mental state during rest, particularly systematic differences related to autism in how the "resting" task is performed, might contribute to our results rather than underlying structural connectivity differences. Because performing an explicit task might reduce interindividual variation in mental state, methods such as using the correlation of residual fluctuations when the effects of task-related activation are removed might provide complementary, albeit still indirect, information about correlated spontaneous neural activity (Jones et al. 2010).

Limitations

Limiting the autism sample to high-functioning males reduces complex heterogeneity prevalent in autism and increases statistical power but does not allow us to determine if the findings extend to females, younger children, and lower functioning individuals with autism. The cross-sectional design limits conclusion about developmental changes but generates hypotheses for longitudinal studies. Measuring interhemispheric correlations at the homologous voxel level results in a huge number of comparisons but allows an anatomically finer grain analysis of case-control differences than permitted by studies that use parcelled cortical areas as ROIs. It is reassuring that both techniques identified similar areas of significant differences between the autism and control samples. The samples we used are limited by the relatively broad age range included. It appears that most of the changes seen with age occur during childhood and adolescence, with relatively few changes after age 20. A more focused study with respect to age might help clarify the timing of changes in interhemispheric correlation. Corpus callosal volumes were calculated with FreeSurfer, which has limited validation on children and adolescent populations included in the present study. Finally, we note that differences seen between autism and control samples are greater for more lateral brain regions but acknowledge that distance from midline is a crude measurement of path length. Future studies might clarify whether this relationship represents medial/lateral axis differences or path length by examining specific connections using probabilistic tractography or other multimodal methods to estimate path length between regions.

Conclusions

The neuroimaging manifestations of autism are widespread with many brain regions implicated. We found decreased interhemispheric correlations between homologous voxels in some but not all regions of the brain in our autism sample relative to controls. Our finding adds to growing evidence that abnormalities of interhemispheric connectivity in autism are widespread but regionally specific and related to cognitive and neurological impairments commonly found in the disorder. Abnormalities in interhemispheric connectivity might be due to a common neural mechanism underlying seemingly disparate aspects of the autism phenotype. Our findings might also be part of a more widespread albeit selective disturbance of spontaneous neuronal activity in autism (Jones et al. 2010).

Interhemispheric connectivity might represent a useful screening method for evaluating neurological disorders where

neural connectivity is implicated in the pathophysiology. Robust interhemispheric connectivity comprises one of the dominant modes of functional connectivity (Stark et al. 2008) and might allow for a simple screening technique for regional differences in connectivity in pathophysiological states. If a different distribution of interhemispheric connectivity abnormalities is seen in other disorders, this would increase confidence that results in this study are not an iceberg effect of generalized connectivity reduction but pathway-specific abnormalities related to neurodevelopmental integration of function in distributed networks.

References

Alexander AL, Lee JE, Lazar M, Boudos R, DuBray MB, Oakes TR, Miller JN, Lu J, Jeong EK, McMahon WM, et al. 2007. Diffusion tensor imaging of the corpus callosum in Autism. Neuroimage. 34:61–73.

American Psychiatric Association 1994. Diagnostic and Statistical Manual of Mental Disorders: DSM-IV. 4th ed. Washington (DC): American Psychiatric Association.

Anderson JS, Druzgal TJ, Lopez-Larson M, Jeong EK, Desai K, Yurgelun-Todd D. 2010. Network anticorrelations, global regression, and phase-shifted soft tissue correction. Hum Brain Mapp. Published Online 9 Jun 2010.

Anderson JS, Lange N, Froehlich A, DuBray M, Druzgal T, Froimowitz M, Alexander A, Bigler E, Lainhart J. 2010. Decreased left posterior insular activity during auditory language in autism. AJNR Am J Neuroradiol. 31:131–139.

Bailey AJ, Braeutigam S, Jousmaki V, Swithenby SJ. 2005. Abnormal activation of face processing systems at early and intermediate latency in individuals with autism spectrum disorder: a magnetoencephalographic study. Eur J Neurosci. 21:2575–2585.

Baron-Cohen S, Ring HA, Wheelwright S, Bullmore ET, Brammer MJ, Simmons A, Williams SC. 1999. Social intelligence in the normal and autistic brain: an fMRI study. Eur J Neurosci. 11:1891–1898.

Bigler ED, Mortensen S, Neeley ES, Ozonoff S, Krasny L, Johnson M, Lu J, Provencal SL, McMahon W, Lainhart JE. 2007. Superior temporal gyrus, language function, and autism. Dev Neuropsychol. 31:217–238.

Birn RM, Diamond JB, Smith MA, Bandettini PA. 2006. Separating respiratory-variation-related fluctuations from neuronal-activity-related fluctuations in fMRI. Neuroimage. 31:1536–1548.

Birn RM, Smith MA, Jones TB, Bandettini PA. 2008. The respiration response function: the temporal dynamics of fMRI signal fluctuations related to changes in respiration. Neuroimage. 40:644–654.

Biswal B, Yetkin FZ, Haughton VM, Hyde JS. 1995. Functional connectivity in the motor cortex of resting human brain using echo-planar MRI. Magn Reson Med. 34:537–541.

Biswal BB, Mennes M, Zuo XN, Gohel S, Kelly C, Smith SM, Beckmann CF, Adelstein JS, Buckner RL, Colcombe S, et al. 2010. Toward discovery science of human brain function. Proc Natl Acad Sci U S A. 107:4734–4739.

Brian J, Bryson SE, Garon N, Roberts W, Smith IM, Szatmari P, Zwaigenbaum L. 2008. Clinical assessment of autism in high-risk 18-month-olds. Autism. 12:433–456.

Brito AR, Vasconcelos MM, Domingues RC, Hygino da Cruz LC, Jr., Rodrigues LD, Gasparetto EL, Calcada CA. 2009. Diffusion tensor imaging findings in school-aged autistic children. J Neuroimaging. 19(4):337–343.

Buckner RL, Sepulcre J, Talukdar T, Krienen FM, Liu H, Hedden T, Andrews-Hanna JR, Sperling RA, Johnson KA. 2009. Cortical hubs revealed by intrinsic functional connectivity: mapping, assessment of stability, and relation to Alzheimer's disease. J Neurosci. 29:1860–1873.

Casanova M, Trippe J. 2009. Radial cytoarchitecture and patterns of cortical connectivity in autism. Philos Trans R Soc Lond B Biol Sci. 364:1433–1436.

Casanova MF, El-Baz A, Mott M, Mannheim G, Hassan H, Fahmi R, Giedd J, Rumsey JM, Switala AE, Farag A. 2009. Reduced gyral window and corpus callosum size in autism: possible macroscopic correlates of a minicolumnopathy. J Autism Dev Disord. 39:751–764.

Castelli F, Frith C, Happe F, Frith U. 2002. Autism, Asperger syndrome and brain mechanisms for the attribution of mental states to animated shapes. Brain. 125:1839–1849.

Cherkassky VL, Kana RK, Keller TA, Just MA. 2006. Functional connectivity in a baseline resting-state network in autism. Neuroreport. 17:1687–1690.

Chung MK, Dalton KM, Alexander AL, Davidson RJ. 2004. Less white matter concentration in autism: 2D voxel-based morphometry. Neuroimage. 23:242–251.

Corbett BA, Carmean V, Ravizza S, Wendelken C, Henry ML, Carter C, Rivera SM. 2009. A functional and structural study of emotion and face processing in children with autism. Psychiatry Res. 173:196–205.

Cordes D, Haughton VM, Arfanakis K, Carew JD, Turski PA, Moritz CH, Quigley MA, Meyerand ME. 2001. Frequencies contributing to functional connectivity in the cerebral cortex in "resting-state" data. AJNR Am J Neuroradiol. 22:1326–1333.

Courchesne E, Pierce K. 2005. Why the frontal cortex in autism might be talking only to itself: local over-connectivity but long-distance disconnection. Curr Opin Neurobiol. 15:225–230.

Dale AM, Fischl B, Sereno MI. 1999. Cortical surface-based analysis. I. Segmentation and surface reconstruction. Neuroimage. 9:179–194.

Dale AM, Sereno MI. 1993. Improved localization of cortical activity by combining EEG and MEG with MRI cortical surface reconstruction: a linear approach. J Cogn Neurosci. 5:162–176.

Desikan RS, Segonne F, Fischl B, Quinn BT, Dickerson BC, Blacker D, Buckner RL, Dale AM, Maguire RP, Hyman BT, et al. 2006. An automated labeling system for subdividing the human cerebral cortex on MRI scans into gyral based regions of interest. Neuroimage. 31:968–980.

Di Martino A, Shehzad Z, Kelly C, Roy AK, Gee DG, Uddin LQ, Gotimer K, Klein DF, Castellanos FX, Milham MP. 2009. Relationship between cingulo-insular functional connectivity and autistic traits in neurotypical adults. Am J Psychiatry. 166:891–899.

Elliott CD. 1990. Differential Ability Scales: Introductory and technical handbook. New York: The Psychological Corporation.

Fair DA, Cohen AL, Dosenbach NU, Church JA, Miezin FM, Barch DM, Raichle ME, Petersen SE, Schlaggar BL. 2008. The maturing architecture of the brain's default network. Proc Natl Acad Sci U S A. 105:4028–4032.

Fair DA, Cohen AL, Power JD, Dosenbach NU, Church JA, Miezin FM, Schlaggar BL, Petersen SE. 2009. Functional brain networks develop

from a "local to distributed" organization. PLoS Comput Biol. 5:e1000381.

Fair DA, Dosenbach NU, Church JA, Cohen AL, Brahmbhatt S, Miezin FM, Barch DM, Raichle ME, Petersen SE, Schlaggar BL. 2007. Development of distinct control networks through segregation and integration. Proc Natl Acad Sci U S A. 104: 13507-13512.

Fischl B, Dale AM. 2000. Measuring the thickness of the human cerebral cortex from magnetic resonance images. Proc Natl Acad Sci U S A. 97:11050-11055.

Fischl B, Liu A, Dale AM. 2001. Automated manifold surgery: constructing geometrically accurate and topologically correct models of the human cerebral cortex. IEEE Trans Med Imaging. 20:70-80.

Fischl B, Salat DH, Busa E, Albert M, Dieterich M, Haselgrove C, van der Kouwe A, Killiany R, Kennedy D, Klaveness S, et al. 2002. Whole brain segmentation: automated labeling of neuroanatomical structures in the human brain. Neuron. 33:341-355.

Fischl B, Salat DH, van der Kouwe AJ, Makris N, Segonne F, Quinn BT, Dale AM. 2004. Sequence-independent segmentation of magnetic resonance images. Neuroimage. 23(Suppl 1):S69-S84.

Fischl B, Sereno MI, Dale AM. 1999. Cortical surface-based analysis. II: inflation, flattening, and a surface-based coordinate system. Neuroimage. 9:195-207.

Fischl B, Sereno MI, Tootell RB, Dale AM. 1999. High-resolution intersubject averaging and a coordinate system for the cortical surface. Hum Brain Mapp. 8:272-284.

Fox MD, Raichle ME. 2007. Spontaneous fluctuations in brain activity observed with functional magnetic resonance imaging. Nat Rev Neurosci. 8:700-711.

Fox MD, Zhang D, Snyder AZ, Raichle ME. 2009. The global signal and observed anticorrelated resting state brain networks. J Neurophysiol. 101:3270-3283.

Freitag CM, Luders E, Hulst HE, Narr KL, Thompson PM, Toga AW, Krick C, Konrad C. 2009. Total brain volume and corpus callosum size in medication-naive adolescents and young adults with autism spectrum disorder. Biol Psychiatry. 66:316-319.

Frith U. 1991. Autism and Asperger syndrome. Cambridge: Cambridge University Press.

Geschwind DH, Levitt P. 2007. Autism spectrum disorders: developmental disconnection syndromes. Curr Opin Neurobiol. 17:103-111.

Gomot M, Bernard FA, Davis MH, Belmonte MK, Ashwin C, Bullmore ET, Baron-Cohen S. 2006. Change detection in children with autism: an auditory event-related fMRI study. Neuroimage. 29:475-484.

Han X, Jovicich J, Salat D, van der Kouwe A, Quinn B, Czanner S, Busa E, Pacheco J, Albert M, Killiany R, et al. 2006. Reliability of MRI-derived measurements of human cerebral cortical thickness: the effects of field strength, scanner upgrade and manufacturer. Neuroimage. 32:180-194.

Hardan AY, Minshew NJ, Keshavan MS. 2000. Corpus callosum size in autism. Neurology. 55:1033-1036.

Jansiewicz EM, Goldberg MC, Newschaffer CJ, Denckla MB, Landa R, Mostofsky SH. 2006. Motor signs distinguish children with high functioning autism and Asperger's syndrome from controls. J Autism Dev Disord. 36:613-621.

Jones TB, Bandettini PA, Kenworthy L, Case LK, Milleville SC, Martin A, Birn RM. 2010. Sources of group differences in functional connectivity: an investigation applied to autism spectrum disorder. Neuroimage. 49(1):401-414.

Jovicich J, Czanner S, Greve D, Haley E, van der Kouwe A, Gollub R, Kennedy D, Schmitt F, Brown G, Macfall J, et al. 2006. Reliability in multi-site structural MRI studies: effects of gradient non-linearity correction on phantom and human data. Neuroimage. 30:436-443.

Just MA, Cherkassky VL, Keller TA, Kana RK, Minshew NJ. 2007. Functional and anatomical cortical underconnectivity in autism: evidence from an FMRI study of an executive function task and corpus callosum morphometry. Cereb Cortex. 17:951-961.

Just MA, Cherkassky VL, Keller TA, Minshew NJ. 2004. Cortical activation and synchronization during sentence comprehension in high-functioning autism: evidence of underconnectivity. Brain. 127:1811-1821.

Kana RK, Keller TA, Cherkassky VL, Minshew NJ, Just MA. 2006. Sentence comprehension in autism: thinking in pictures with decreased functional connectivity. Brain. 129:2484-2493.

Keary CJ, Minshew NJ, Bansal R, Goradia D, Fedorov S, Keshavan MS, Hardan AY. 2009. Corpus callosum volume and neurocognition in autism. J Autism Dev Disord. 39:834-841.

Keller TA, Kana RK, Just MA. 2007. A developmental study of the structural integrity of white matter in autism. Neuroreport. 18:23-27.

Kennedy DP, Courchesne E. 2008. The intrinsic functional organization of the brain is altered in autism. Neuroimage. 39:1877-1885.

Kennedy DP, Redcay E, Courchesne E. 2006. Failing to deactivate: resting functional abnormalities in autism. Proc Natl Acad Sci U S A. 103:8275-8280.

Kleinhans NM, Richards T, Sterling L, Stegbauer KC, Mahurin R, Johnson LC, Greenson J, Dawson G, Aylward E. 2008. Abnormal functional connectivity in autism spectrum disorders during face processing. Brain. 131:1000-1012.

Koshino H, Carpenter PA, Minshew NJ, Cherkassky VL, Keller TA, Just MA. 2005. Functional connectivity in an fMRI working memory task in high-functioning autism. Neuroimage. 24:810-821.

Koshino H, Kana RK, Keller TA, Cherkassky VL, Minshew NJ, Just MA. 2008. fMRI investigation of working memory for faces in autism: visual coding and underconnectivity with frontal areas. Cereb Cortex. 18:289-300.

Kraemer HC, Yesavage JA, Taylor JL, Kupfer D. 2000. How can we learn about developmental processes from cross-sectional studies, or can we? Am J Psychiatry. 157:163-171.

Lainhart J, Lazar M, Bigler E, Alexander A. 2005. Advances in neuroimaging: looking into the brain in autism. In: Casanova M, editor. Recent developments in autism research. New York: Nova Science Publishers, Inc. p. 57-108.

Lee JE, Bigler ED, Alexander AL, Lazar M, DuBray MB, Chung MK, Johnson M, Morgan J, Miller JN, McMahon WM, et al. 2007. Diffusion tensor imaging of white matter in the superior temporal gyrus and temporal stem in autism. Neurosci Lett. 424:127-132.

Lee PS, Yerys BE, Della Rosa A, Foss-Feig J, Barnes KA, James JD, VanMeter J, Vaidya CJ, Gaillard WD, Kenworthy LE. 2009. Functional connectivity of the inferior frontal cortex changes with age in children with autism spectrum disorders: a fcMRI study of response inhibition. Cereb Cortex. 19:1787-1794.

Leyfer OT, Folstein SE, Bacalman S, Davis NO, Dinh E, Morgan J, Tager-Flusberg H, Lainhart JE. 2006. Comorbid psychiatric disorders in children with autism: interview development and rates of disorders. J Autism Dev Disord. 36:849-861.

Lord C, Risi S, Lambrecht L, Cook EH Jr, Leventhal BL, DiLavore PC, Pickles A, Rutter M. 2000. The autism diagnostic observation schedule-generic: a standard measure of social and communication deficits associated with the spectrum of autism. J Autism Dev Disord. 30:205-223.

Lord C, Rutter M, Le Couteur A. 1994. Autism Diagnostic Interview-Revised: a revised version of a diagnostic interview for caregivers of individuals with possible pervasive developmental disorders. J Autism Dev Disord. 24:659-685.

Lowe MJ, Mock BJ, Sorenson JA. 1998. Functional connectivity in single and multislice echoplanar imaging using resting-state fluctuations. Neuroimage. 7:119-132.

Maldjian JA, Laurienti PJ, Kraft RA, Burdette JH. 2003. An automated method for neuroanatomic and cytoarchitectonic atlas-based interrogation of fMRI data sets. Neuroimage. 19:1233-1239.

Manes F, Piven J, Vrancic D, Nanclares V, Plebst C, Starkstein SE. 1999. An MRI study of the corpus callosum and cerebellum in mentally retarded autistic individuals. J Neuropsychiatry Clin Neurosci. 11:470-474.

Mason RA, Williams DL, Kana RK, Minshew N, Just MA. 2008. Theory of mind disruption and recruitment of the right hemisphere during narrative comprehension in autism. Neuropsychologia. 46: 269-280.

Monk CS, Peltier SJ, Wiggins JL, Weng SJ, Carrasco M, Risi S, Lord C. 2009. Abnormalities of intrinsic functional connectivity in autism spectrum disorders. Neuroimage. 47:764-772.

Mostofsky SH, Burgess MP, Gidley Larson JC. 2007. Increased motor cortex white matter volume predicts motor impairment in autism. Brain. 130:2117-2122.

Mostofsky SH, Powell SK, Simmonds DJ, Goldberg MC, Caffo B, Pekar JJ. 2009. Decreased connectivity and cerebellar activity in autism during motor task performance. Brain. 132:2413-2425.

Muller RA, Kleinhans N, Kemmotsu N, Pierce K, Courchesne E. 2003. Abnormal variability and distribution of functional maps in autism: an FMRI study of visuomotor learning. Am J Psychiatry. 160:1847-1862.

Murphy K, Birn RM, Handwerker DA, Jones TB, Bandettini PA. 2009. The impact of global signal regression on resting state correlations: are anti-correlated networks introduced? Neuroimage. 44:893-905.

Oldfield RC. 1971. The assessment and analysis of handedness: the Edinburgh inventory. Neuropsychologia. 9:97-113.

Oram Cardy JE, Flagg EJ, Roberts W, Brian J, Roberts TP. 2005. Magnetoencephalography identifies rapid temporal processing deficit in autism and language impairment. Neuroreport. 16:329-332.

Pierce K, Redcay E. 2008. Fusiform function in children with an autism spectrum disorder is a matter of "who". Biol Psychiatry. 64:552-560.

Scheperjans F, Eickhoff SB, Homke L, Mohlberg H, Hermann K, Amunts K, Zilles K. 2008. Probabilistic maps, morphometry, and variability of cytoarchitectonic areas in the human superior parietal cortex. Cereb Cortex. 18:2141-2157.

Seeley WW, Menon V, Schatzberg AF, Keller J, Glover GH, Kenna H, Reiss AL, Greicius MD. 2007. Dissociable intrinsic connectivity networks for salience processing and executive control. J Neurosci. 27:2349-2356.

Segonne F, Dale AM, Busa E, Glessner M, Salat D, Hahn HK, Fischl B. 2004. A hybrid approach to the skull stripping problem in MRI. Neuroimage. 22:1060-1075.

Segonne F, Pacheco J, Fischl B. 2007. Geometrically accurate topology-correction of cortical surfaces using nonseparating loops. IEEE Trans Med Imaging. 26:518-529.

Semel E, Wiig EH, Secord WA. 1995. Clinical evaluation of language fundamentals—3rd edition (CELF-3). San Antonio (TX): Psychological Corporation.

Sled JG, Zijdenbos AP, Evans AC. 1998. A nonparametric method for automatic correction of intensity nonuniformity in MRI data. IEEE Trans Med Imaging. 17:87-97.

Stanfield AC, McIntosh AM, Spencer MD, Philip R, Gaur S, Lawrie SM. 2008. Towards a neuroanatomy of autism: a systematic review and meta-analysis of structural magnetic resonance imaging studies. Eur Psychiatry. 23:289-299.

Stark DE, Margulies DS, Shehzad ZE, Reiss P, Kelly AM, Uddin LQ, Gee DG, Roy AK, Banich MT, Castellanos FX, et al. 2008. Regional variation in interhemispheric coordination of intrinsic hemodynamic fluctuations. J Neurosci. 28:13754-13764.

Stevens MC, Pearlson GD, Calhoun VD. 2009. Changes in the interaction of resting-state neural networks from adolescence to adulthood. Hum Brain Mapp. 30:2356-2366.

Supekar K, Musen M, Menon V. 2009. Development of large-scale functional brain networks in children. PLoS Biol. 7:e1000157.

Tzourio-Mazoyer N, Landeau B, Papathanassiou D, Crivello F, Etard O, Delcroix N, Mazoyer B, Joliot M. 2002. Automated anatomical labeling of activations in SPM using a macroscopic anatomical parcellation of the MNI MRI single-subject brain. Neuroimage. 15:273-289.

Uddin LQ, Menon V. 2009. The anterior insula in autism: under-connected and under-examined. Neurosci Biobehav Rev. 33(8):1198-1203.

van Kooten IA, Palmen SJ, von Cappeln P, Steinbusch HW, Korr H, Heinsen H, Hof PR, van Engeland H, Schmitz C. 2008. Neurons in the fusiform gyrus are fewer and smaller in autism. Brain. 131:987-999.

Varela F, Lachaux JP, Rodriguez E, Martinerie J. 2001. The brainweb: phase synchronization and large-scale integration. Nat Rev Neurosci. 2:229-239.

Vidal CN, Nicolson R, DeVito TJ, Hayashi KM, Geaga JA, Drost DJ, Williamson PC, Rajakumar N, Sui Y, Dutton RA, et al. 2006. Mapping corpus callosum deficits in autism: an index of aberrant cortical connectivity. Biol Psychiatry. 60:218-225.

Vilensky JA, Damasio AR, Maurer RG. 1981. Gait disturbances in patients with autistic behavior: a preliminary study. Arch Neurol. 38:646-649.

Waiter GD, Williams JH, Murray AD, Gilchrist A, Perrett DI, Whiten A. 2005. Structural white matter deficits in high-functioning individuals with autistic spectrum disorder: a voxel-based investigation. Neuroimage. 24:455-461.

Wechsler D. 1997. Wechsler Adult Intelligence Scale—Third Edition (WAIS-III). San Antonio (TX): The Psychological Corporation.

Wechsler D. 1999. Wechsler Abbreviated Scale of Intelligence (WASI). San Antonio (TX): The Psychological Corporation.

Weng SJ, Wiggins JL, Peltier SJ, Carrasco M, Risi S, Lord C, Monk CS. 2009. Alterations of resting state functional connectivity in the default network in adolescents with autism spectrum disorders. Brain Res. 1313:202-214.

Wilson TW, Rojas DC, Reite ML, Teale PD, Rogers SJ. 2007. Children and adolescents with autism exhibit reduced MEG steady-state gamma responses. Biol Psychiatry. 62:192-197.

Zuo XN, Kelly C, Di Martino A, Mennes M, Margulies DS, Bangaru S, Grzadzinski R, Evans AC, Zang YF, Castellanos FX, et al. 2010. Growing together and growing apart: Regional differences in the lifespan developmental trajectories of functional homotopy. J Neurosci. (forthcoming).

Zwaigenbaum L, Bryson S, Lord C, Rogers S, Carter A, Carver L, Chawarska K, Constantino J, Dawson G, Dobkins K, et al. 2009. Clinical assessment and management of toddlers with suspected autism spectrum disorder: insights from studies of high-risk infants. Pediatrics. 123:1383-1391.